Title

Dynamic variability of biogeochemical ratios in the Southern California Current System

Journal

Geophysical Research Letters, 41(7)

ISSN

0094-8276

Authors

Martz, Todd
Send, Uwe
Ohman, Mark D
et al.

Publication Date

2014-04-16

DOI

10.1002/2014gl059332

Peer reviewed

AGU PUBLICATIONS

Geophysical Research Letters

RESEARCH LETTER
10.1002/2014GL059332

Key Points:
- Chemical sensors provide a means to observe the Redfield ratios
- Redfield ratios vary on the weekly timescale
- The f ratio ranges from 100% New to 100% Regenerated Production

Supporting Information:
- Response to Reviewer_AM
- ReadMe
- Figure S1
- Figure S2
- Figure S3
- Figure S4
- Figure S5

Correspondence to:
T. Martz,
trmartz@ucsd.edu

Citation:
Martz, T., U. Send, M. D. Ohman, Y. Takeshita, P. Bresnahan, H.-J. Kim, and S. H. Nam (2014), Dynamic variability of biogeochemical ratios in the Southern California Current System, *Geophys. Res. Lett.*, *41*, 2496–2501, doi:10.1002/2014GL059332.

Received 17 JAN 2014
Accepted 20 MAR 2014
Accepted article online 21 MAR 2014
Published online 14 APR 2014

Dynamic variability of biogeochemical ratios in the Southern California Current System

Todd Martz[1], Uwe Send[1], Mark D. Ohman[1], Yuichiro Takeshita[1], Philip Bresnahan[1], Hey-Jin Kim[1], and SungHyun Nam[1]

[1]Scripps Institution of Oceanography, University of California, San Diego, La Jolla, California, USA

Abstract We use autonomous nitrate (NO_3^-), oxygen (O_2), and dissolved inorganic carbon (DIC) observations to examine the relationship between ratios of C:N:O at an upwelling site in the Southern California Current System. Mean ratios and 95% confidence intervals observed by sensors over 8 months were NO_3^-:O_2 = −0.11 ± 0.002, NO_3^-:DIC = 0.14 ± 0.001, and DIC:O_2 = −0.83 ± 0.01, in good agreement with Redfield ratios. Variability in the ratios on the weekly time scale is attributable to shifts in biological demand and nutrient availability and shown to exhibit a spectrum of values ranging from near 100% New Production to 100% Regenerated Production.

1. Introduction

Over the past decade, chemical sensors have provided new insight into biogeochemical variability [*Johnson et al.*, 2007], carbon budgets in the open ocean [*DeGrandpre et al.*, 2004; *Emerson and Stump*, 2010; *Emerson et al.*, 2008, 2011; *Körtzinger et al.*, 2008a, 2008b; *Martz et al.*, 2009], and the stoichiometric relationships between dissolved inorganic carbon (DIC), oxygen (O_2), and nitrate (NO_3^-) [*Johnson*, 2010; *Körtzinger et al.*, 2008b]. As the technologies mature, colocated chemical sensors will become more commonplace on a variety of platforms [*Johnson et al.*, 2009; *Ohman et al.*, 2013], providing new opportunities to examine properties such as the "Redfield ratio" [*Redfield*, 1934] and the "*f* ratio" [*Eppley and Peterson*, 1979] with spatiotemporal resolution unavailable to the originators of these classic concepts.

Since Redfield's work [*Redfield*, 1934], the idea of near-constant element ratios in plankton driving the composition of seawater has become a cornerstone of ocean biogeochemistry. The idea has since matured to recognize regional, ecosystem, and species-dependent differences in the traditional ratio of 106C:16N:1P:−138O_2 that is often expressed as a hypothetical chemical reaction

$$106CO_2 + 16HNO_3 + 1H_3PO_4 + 122H_2O \rightleftharpoons (CH_2O)_{106}(NH_3)_{16}H_3PO_4 + 138O_2 \quad (1)$$

These ratios have been observed to vary over depth and by location in terms of both the composition of sinking organic matter [*Martin et al.*, 1987; *Martiny et al.*, 2013] and composition of dissolved species in the seawater [*Anderson and Sarmineto*, 1994; *Deutsch and Weber*, 2012]. They have also been observed to vary over a fairly wide range in culture studies [*Geider and La Roche*, 2002].

Another fundamental concept of ocean biogeochemistry distinguishes New (or nitrate-plus fixed dinitrogen-fueled) Production (equation (1)) from Regenerated Production in which reduced forms of nitrogen such as NH_4^+ substitute for HNO_3 in equation (1) [*Dugdale and Goering*, 1967]. The so-called *f* ratio is defined as the fraction of New/Total (New + Regenerated) Production [*Eppley and Peterson*, 1979]. The present state of chemical sensor technology readily allows high quality continuous observation of the dissolved seawater concentrations of three terms in equation (1): CO_2, HNO_3, and O_2. Here we utilize such information in the context of Redfield ratios and New versus Regenerated Production to resolve dynamic variations in these properties.

2. Observations

2.1. Moorings and Study Site

The CCE-2 mooring (Figure S1 in the supporting information) is operated at 120.7°W, 34.2°N, ~35 km off Point Conception in the California Current Ecosystem Long Term Ecological Research (CCE-LTER) site. The mooring

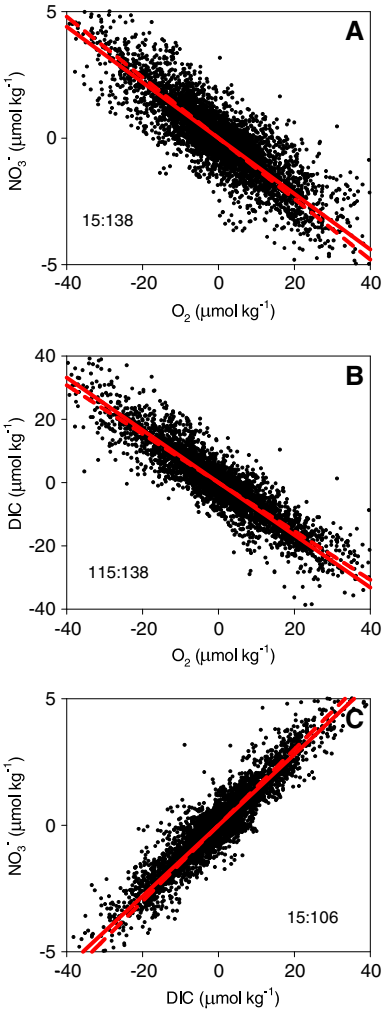

Figure 1. (a–c) Property-property plots of 33 h high-pass filtered NO_3^-, DIC, and O_2 at CCE-2 (black dots). Lines are shown for the slope of a Type II regression (solid red, slope indicated in panel) and Redfield ratios (dashed red).

is positioned on the continental slope and inshore of the core of the California Current, a broad equatorward surface flow that parallels the coastline between ~100 and 300 km offshore. At CCE-2, local upwelling and advection strongly influence water properties. It is noteworthy that this mooring is located in one of the best studied regions of the coastal ocean, covered by the overlapping California Cooperative Oceanic Fisheries Investigations and CCE-LTER sites, which provide a wealth of historical data from time series and process cruises. The time series discussed in this work spans a 237 day period from 9 March to 1 November 2011.

2.2. Elemental Ratios from High-Pass Filtered Data

Similar to *Johnson* [2010], sensor data for DIC, O_2, and NO_3^- were processed using a 33 h high-pass filter (Matlab, zero phase fifth order Butterworth). DIC is computed from pH sensor data using regional relationships of total alkalinity [*Alin et al.*, 2012]. Further details of data processing and QC are provided in the supporting information.

The resulting time series contains variability due to daily production and respiration and mixing associated with processes such as diel changes in mixed layer depth. The effects of lower frequency processes such as upwelling and relaxation are largely removed by the high-pass filter. As described by *Johnson* [2010], the filtered time series contains information on the local stoichiometric relationship between carbon, oxygen, and nitrogen. Uptake/remineralization ratios were calculated using a Type II regression for the filtered time series as a whole and piecewise using a shifting 5 day window to examine temporal variability.

3. Results and Discussion

Over the 8 months, the sea surface warmed by ~4°C, the mixed layer depth shoaled from ~60 m in March to ~20 m after June and five prominent low-oxygen, high-DIC events were observed (Figure S2). Comparison with the along-shore current indicates that some events are due to direct upwelling at the mooring site while others are likely the result of advection of water upwelled nearby. Although no smooth seasonal pattern is observed at CCE-2, the frequency of high-DIC low-O_2 events undergoes a marked shift after June. In the first 4 months of the time series, the frequency of persistent upwelling events is ~1 mo^{-1}; but only one major event is observed during the last 4 months.

3.1. Elemental Ratios From High-Pass Filtered Data

The relationships between high-pass filtered NO_3^-, O_2, and DIC are presented in Figure 1 and Table 1. The very close agreement between the overall mean slopes and the Redfield ratios (Table 1) confirms that variability isolated by the temporal filter is largely due to biological processes.

Divergence of the sensor data from the Redfield ratio is possible through several different processes. As mentioned above, significant regional differences in particle C:P and C:N ratios have been observed and attributed to differences in phytoplankton lineage [*Martiny et al.*, 2013]. Deviations in DIC:O_2 may result from gas exchange, as O_2 equilibrates with the atmosphere more rapidly than CO_2. This leads to reduced amplitude in the filtered oxygen data, forcing the slope in Figure 1b to a more negative value than the

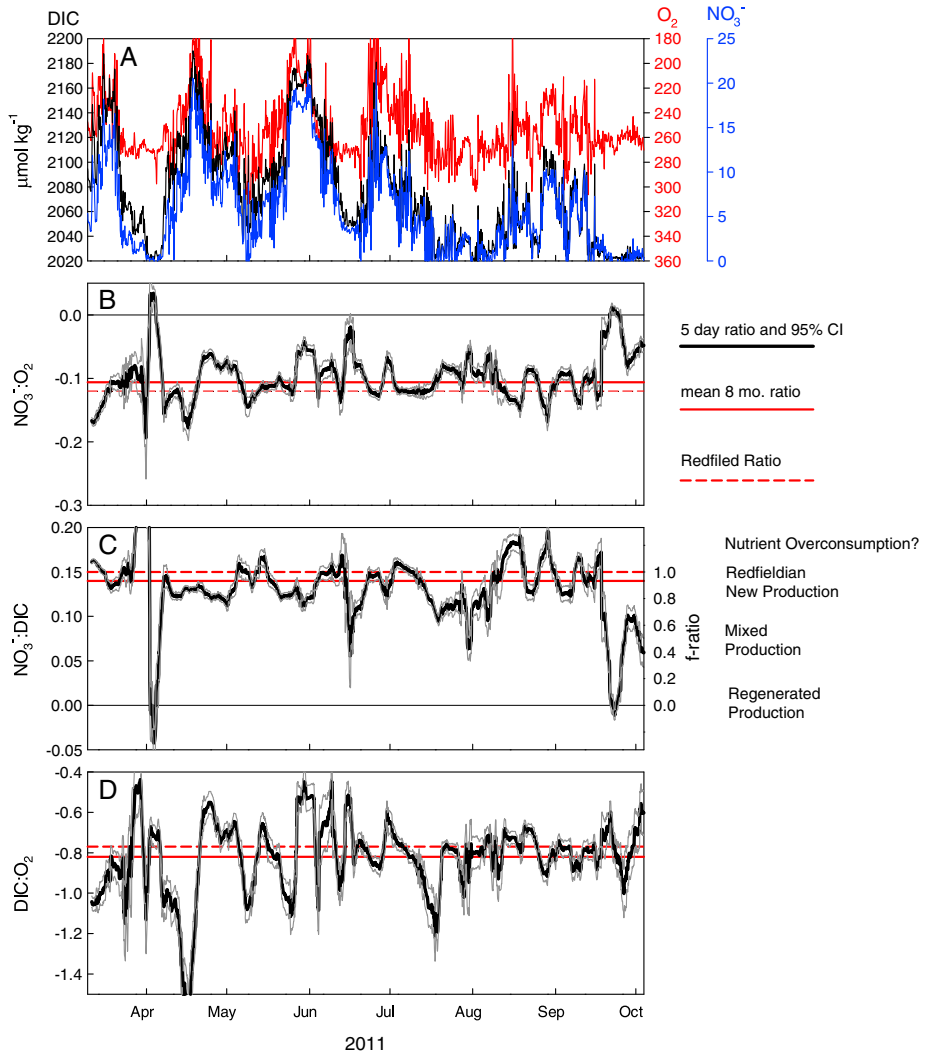

Figure 2. (a) Unfiltered NO_3^-, DIC, and O_2 dynamics at CCE-2 during 2011. (b–d) Ratios of 33 h high-pass filtered data from Figure 2a, using a 5 day window. Grey lines are 95% CIs.

Redfield ratio. Both the NO_3^-:DIC and NO_3^-:O_2 ratios (Figures 1a and 1c) are affected by the source of nitrogen taken up by phytoplankton. NO_3^-:O_2 is also affected by O_2 gas exchange. However, the close agreement between Redfield values and both ratios involving NO_3^- (Table 1) suggests little (<10%) Regenerated Production at CCE-2. In other words, the *f* ratio [*Eppley and Peterson*, 1979] computed by combining the sensor data with Redfield ratios is close to 1. It is noteworthy that *Johnson* [2010] observed very different ratios in Monterey Bay, CA, using similar sensors and data processing. For comparison, these numbers are included in Table 1. In his study, Johnson concluded that O_2 gas exchange and Regenerated Production were the sources of the discrepancy. Both studies were carried out during overlapping portions of

Table 1. Ratios of 33 h High-Pass Filtered Data

Redfield Ratio	Ratio	CCE-2	M1[a]	M2[a]
(16N:138O_2) −0.12	NO_3^-:O_2	−0.11 ± 0.002	−0.095	−0.076
(16N:106 CO_2) 0.15	NO_3^-:DIC	0.14 ± 0.001	0.073	0.071
(106CO_2:138O_2) −0.77	DIC:O_2	−0.83 ± 0.01	−1.3	−1.1

[a]Values reported in *Johnson* [2010, Table 1].

the year and in similar regimes, characteristic of upwelling, high nutrients, and high productivity, and both exhibited nearly identical ranges of NO_3^-, DIC, and O_2. One difference between the two studies is the depth of the sensor packages. On the Monterey moorings, all sensors were located within ~1 m of the surface but on CCE-2, sensors were located between 15 and 17 m below the surface. Although the mixed layer depth was often deeper than 15 m, the subsurface sensors showed consistently lower O_2 and higher DIC (Figure S3), suggesting some combination of isolation from the atmosphere, enhanced mixing, and less productivity at depth. This may explain some of the difference between our ratios involving O_2 and those reported by *Johnson* [2010], yet DIC is insensitive to gas exchange on the 33 h time scale, so gas exchange cannot explain the differences in the NO_3^-:DIC. If NO_3^- and DIC variability at 15 m is driven by the same processes as the surface, the difference in the ratios observed in Monterey Bay in comparison with CCE-2 may be due to real differences in the *f* ratio.

3.2. Temporal Evolution of Elemental Ratios

In Figure 2 we examine the dynamics underlying the scatter in Figure 1 by computing the same Type II regressions shown in Figure 1 over a moving 5 day window. Several high-nutrient events are apparent (Figure 2a), corresponding to nearby upwelling. The 33 h high-pass filter removes these events, isolating the local biological uptake and respiration signals associated with the diel cycle. Short-term mixing such as nighttime deepening of the mixed layer will also affect the filtered results with a similar local biological signal reflecting the properties of the subsurface pools of DIC, NO_3^-, and O_2. Temporal dynamics in Figures 2b–2d therefore reflect a mean stoichiometric ratio specific to CCE-2 over a 5 day window. The maximum daily amplitudes of filtered DIC, O_2, and NO_3^- observed in this study (corresponding to the axis ranges in Figure 1) are similar to those reported by *Johnson* [2010]. Amplitudes ranged from these maximum values to minima roughly 10 times smaller (Figure S4). It is important to note that daily amplitude is not a measure of net ecosystem metabolism. Calculation of the latter from the mooring data requires a budget approach that properly accounts for physical processes and will be the subject of a future study.

The pH and O_2 sensors are capable of resolving changes smaller than 1 μmol kg^{-1} for DIC and O_2; thus, it can be reasonably stated that the high-pass filtered data seldom approach detection limits of these sensors. During periods where NO_3^- reaches levels near the sensor's detection limit (2 μM), the amplitude of high-pass filtered NO_3^- approaches zero while DIC and O_2 amplitude always remain nonzero and detectable at levels higher than the corresponding limit of the NO_3^- sensor, effectively driving the ratios in Figures 2b and 2c toward the zero line and indicating an alternative source of nitrogen.

Environmental variables with an upwelling signature such as temperature and density correlate with the temporal variability seen in Figure 2a (Figure S2). However, much of this correlation is lost in the 5 day ratio (Figures 2b–2d). Examination of Figures 2 and S2 reveals a correspondence between NO_3^- level, amplitude of high-pass filtered data, and the elemental ratios such that freshly upwelled water approaches Redfieldian values and experiences high amplitudes, whereas NO_3^--depleted waters tend to diverge from the Redfield ratio.

Following Figure 2c, we identify four regimes: Redfieldian New Production, Mixed Production (i.e., significant New and Regenerated Production are present), Regenerated Production, and Nutrient Overconsumption. These regimes are most prominent in Figure 2c because O_2 gas exchange does not complicate the ratio. In Figures 2b and 2c the transition from New to Mixed Production is identified as a departure from the dashed line (the traditional Redfield ratio) toward the zero line (100% Regenerated Production). Two events are apparent where NO_3^-:DIC approaches zero, indicating periods dominated almost exclusively by Regenerated Production (Figure 2c). A fourth regime: Nutrient Overconsumption may have occurred during periods where NO_3^-:DIC exceeds the Redfield ratio (Figure 2c). In spite of decreasing frequency of nutrient delivery (Figure 2a), there is no overall trend in the NO_3^-:O_2 and NO_3^-:DIC that would suggest a broadscale transition from New to Regenerated Production (Figures 2b and 2c). However, during this time there are a number of transitions on the order of 20–30% of the ratio. It is particularly encouraging that the upper and lower limits of the NO_3^-:DIC ratio coincide with the theoretical bounds of 100% Redfieldian New Production and 0% New Production (100% Regenerated Production). In the analysis presented here we do not attempt to assess a lag time between nutrient delivery, bloom, and postbloom dynamics because the events captured at the moorings are transient and represent water masses with variable time history since upwelling. Still, it may be

feasible in future work to combine additional data sets (e.g., chlorophyll *a* fluorescence, currents, spatial gradients) to better understand the timing of these processes. Dynamics of the ratios on weekly scales (Figure 2) may be responsible for the differences observed between CCE-2 and Monterey, although *Johnson* [2010] did not report ratios on the weekly time scale. For example, the 5 month time series in Monterey Bay exhibited 1–2 high-DIC low-O_2 events compared to three events over the same 5 months of the year at CCE-2. High- versus low-nutrient conditions clearly influence the computed ratios, the number of excursions toward Regenerated Production (Figure 2c), and ultimately the overall slope calculated for the time series as a whole.

It was recognized by Redfield that uptake ratios are organism dependent and the imprint left on the water mass due to remineralization of organic matter represents an average. Treating the Redfield ratios as global or regional constants may be acceptable in the context of interpreting snapshots of the water column captured in shipboard bottle data [*Anderson and Sarmineto*, 1994], but extending these assumptions to high temporal resolution data captured by autonomous platforms presents a new problem that has received little attention. In particular, the extreme shifts in species dominance characteristic of high-productivity regions must lead to some measure of variability in the uptake/remineralization ratios [*Geider and La Roche*, 2002]. Similar to the Redfield ratio, it was established at the outset that the *f* ratio is variable [*Eppley and Peterson*, 1979], although it too, by necessity, is oversimplified in global modeling studies [*Dunne et al*., 2005]. Both ratios have been coarsely mapped, yet little information exists on the temporal evolution of either variable, particularly at the scales shown in Figure 2. The observations presented here provide compelling evidence of dynamic elemental ratios and export production (implied by a variable *f* ratio). In the future, data returned by autonomous sensors in the ocean should be interpreted with such variability in mind. In summary, Redfield ratios from deep water chemical concentrations and pelagic Photosynthetic and Respiratory Quotients derive from different processes [*Williams and Robertson*, 1991; *Laws*, 1991; *Sakshaug et al*., 1997], making it critical that appropriate stoichiometric ratios are used to interpret sensor data, or conversely that sensors are necessary in order to appreciate the breadth of plankton stoichiometry in the ocean.

4. Conclusions

Autonomous chemical sensors allow calculation of elemental uptake and remineralization ratios on time scales previously not studied at the ecosystem level. Although the long-term mean relationships agree quite well with traditional Redfield ratios, close examination of the sensor data at daily to weekly time scales reveals dynamic changes reflecting ecosystem level processes such as shifts in the *f* ratio or in species dominance.

Acknowledgments

The CCE mooring program is a team effort between multiple labs and principal investigators at Scripps Institution, the NOAA PMEL carbon and ocean acidification group, the NOAA Southwest Fisheries Science Center, and UC Santa Barbara. The mooring design, deployments, and operation are the results of dedicated and highly professional work of the Send mooring team at SIO together with the operators and crews of the SIO research vessels. Support for the CCE mooring work is provided by the NOAA Ocean Acidification Program, the NOAA Climate Observation Division, and the NOAA National Marine Fisheries Service. Partial support was also provided from NSF via the California Current Ecosystem LTER site (Ohman) and the UC San Diego Foundation (Martz). Data used in the manuscript are available upon request to the corresponding author (trmartz@ucsd.edu).

The Editor thanks Adam Martiny and an anonymous reviewer for their assistance in evaluating this paper.

References

Alin, S. R., R. A. Feely, A. G. Dickson, J. M. Hernández-Ayón, L. W. Juranek, M. D. Ohman, and R. Goericke (2012), Robust empirical relationships for estimating the carbonate system in the southern California Current System and application to CalCOFI hydrographic cruise data, *J. Geophys. Res.*, *117*, C05033, doi:10.1029/2011JC007511.

Anderson, L. A., and J. L. Sarmineto (1994), Redfield ratios of remineralization determined by nutrient data analysis, *Global Biogeochem. Cycles*, *8*(1), 65–80.

DeGrandpre, M. D., R. Wanninkhof, W. R. McGillis, and P. G. Strutton (2004), A Lagrangian study of surface pCO_2 dynamics in the eastern equatorial Pacific Ocean, *J. Geophys. Res.*, *109*, C08S07, doi:10.1029/2003JC002089.

Deutsch, C., and T. Weber (2012), Nutrient ratios as a tracer and driver of ocean biogeochemistry, *Annu. Rev. Mar. Sci.*, *4*(1), 113–141.

Dugdale, R. C., and J. J. Goering (1967), Uptake of new and regenerated forms of nitrogen in primary productivity, *Limnol. Oceanogr.*, *12*(2), 196–206.

Dunne, J. P., R. A. Armstrong, A. Gnanadesikan, and J. L. Sarmiento (2005), Empirical and mechanistic models for the particle export ratio, *Global Biogeochem. Cycles*, *19*, GB4026, doi:10.1029/2004GB002390.

Emerson, S., and C. Stump (2010), Net biological oxygen production in the ocean—II: Remote in situ measurements of O_2 and N_2 in subarctic pacific surface waters, *Deep Sea Res., Part I*, *57*(10), 1255–1265.

Emerson, S., C. Stump, and D. Nicholson (2008), Net biological oxygen production in the ocean: Remote in situ measurements of O_2 and N_2 in surface waters, *Global Biogeochem. Cycles*, *22*, GB3023, doi:10.1029/2007GB003095.

Emerson, S., C. Sabine, M. F. Cronin, R. Feely, S. E. Cullison Gray, and M. DeGrandpre (2011), Quantifying the flux of $CaCO_3$ and organic carbon from the surface ocean using in situ measurements of O_2, N_2, pCO_2, and pH, *Global Biogeochem. Cycles*, *25*, GB3008, doi: 10.1029/2010GB003924.

Eppley, R. W., and B. J. Peterson (1979), Particulate organic matter flux and planktonic new production in the deep ocean, *Nature*, *282*(5740), 677–680.

Geider, R., and J. La Roche (2002), Redfield revisited: Variability of C:N:P in marine microalgae and its biochemical basis, *Eur. J. Phycol.*, *37*(1), 1–17.

Johnson, K. S. (2010), Simultaneous measurements of nitrate, oxygen, and carbon dioxide on oceanographic moorings: Observing the Redfield Ratio in real time, *Limnol. Oceanogr.*, *55*(2), 615–627.

Johnson, K. S., J. A. Needoba, S. C. Riser, and W. J. Showers (2007), Chemical sensor networks for the aquatic environment, *Chem. Rev.*, *107*(2), 623–640.

Johnson, K. S., W. M. Berelson, E. S. Boss, Z. Chase, H. Claustre, S. R. Emerson, N. Gruber, A. Kortzinger, M. J. Perry, and S. C. Riser (2009), Observing biogeochemical cycles at global scales with profiling floats and gliders: Prospects for a global array, *Oceanography*, *22*(3), 216–225.

Körtzinger, A., U. Send, D. Wallace, J. Karstensen, and M. DeGrandpre (2008a), Seasonal cycle of O_2 and pCO_2 in the central Labrador Sea: Atmospheric, biological, and physical implications, *Global Biogeochem. Cycles*, *22*, GB1014, doi:10.1029/2007GB003029.

Körtzinger, A., U. Send, R. S. Lampitt, S. Hartman, D. W. R. Wallace, J. Karstensen, M. G. Villagarcia, O. Llinas, and M. D. DeGrandpre (2008b), The seasonal pCO2 cycle at 49°N/16.5°W in the northeastern Atlantic Ocean and what it tells us about biological productivity, *J. Geophys. Res.*, *113*, C04020, doi:10.1029/2007JC004347.

Laws, E. A. (1991), Photosynthetic quotients, new production and net community production in the open ocean, *Deep-Sea Res. Part A*, *38*(1A), 143–167.

Martin, J. H., G. A. Knauer, D. M. Karl, and W. W. Broenkow (1987), VERTEX: Carbon cycling in the northeast Pacific, *Deep-Sea Res. Part A*, *34*(2A), 267–285.

Martiny, A. C., C. T. A. Pham, F. W. Primeau, J. A. Vrugt, J. K. Moore, S. A. Levin, and M. W. Lomas (2013), Strong latitudinal patterns in the elemental ratios of marine plankton and organic matter, *Nat. Geosci.*, *6*(4), 279–283.

Martz, T. R., M. D. DeGrandpre, P. G. Strutton, W. R. McGillis, and W. M. Drennan (2009), Sea surface pCO_2 and carbon export during the Labrador Sea spring-summer bloom: An in situ mass balance approach, *J. Geophys. Res.*, *114*, C09008, doi:10.1029/2008JC005060.

Ohman, M. D., D. L. Rudnick, A. Chekalyuk, R. E. Davis, R. A. Feely, M. Kahru, H.-J. Kim, M. R. Landry, T. R. Martz, and C. L. Sabine (2013), Autonomous ocean measurements in the California Current Ecosystem, *Oceanography*, *26*(3), 18–25.

Redfield, A. C. (1934), On the proportion of organic derivatives in sea water and their relation to the composition of plankton, in *James Johnstone Memorial Volume*, pp. 177–192, Liverpool Univ. Press, Liverpool, U. K.

Sakshaug, E., A. Bricaud, Y. Dandonneau, P. G. Falkowski, D. A. Kiefer, L. Legendre, A. Morel, J. Parslow, and M. Takahashi (1997), Parameters of photosynthesis: Definitions, theory and interpretation of results, *J. Plankton Res.*, *19*(11), 1637–1670.

Williams, P. J. I., and J. E. Robertson (1991), Overall planktonic oxygen and carbon dioxide metabolisms: The problem of reconciling observations and calculations of photosynthetic quotients, *J. Plankton Res.*, *13*(supp1), 153–169.